MODELLING OF PLANFORM INFLUENCE ON CIRCULATION IN HARBOURS

by

ROGER A. FALCONER*

ABSTRACT

A two dimensional numerical model has been developed which is capable of predicting the tidal water elevations, depth averaged velocity components and horizontal concentration distributions in narrow entranced harbours and marinas. Particular attention has been paid to the numerical treatment of the convective accelerations where, as a result of narrow harbour entrances and the general nature of planform geometries, the resulting highly non-uniform flow fields can readily lead to non-linear instabilities and unstable numerical solutions.

In order to check the validity of the numerical results, a comprehensive study was carried out to compare, with scaled laboratory model studies, the predicted tidal velocity fields and flushing characteristics for a number of rectangular harbours of constant planform area but different length to breadth ratios. The experimentally measured average per cycle exchange coefficients and the observed mean water level pathlines agreed reasonably well with the corresponding numerically predicted exchange coefficients and depth averaged velocity fields.

The results of both the numerical and laboratory model studies confirmed conclusively that the maximum gross flushing characteristics occurred within a rectangular harbour when the length to breadth ratio was close to unity. Also, further tests showed that the insertion of impermeable barriers as a possible means of increasing the flushing efficiency proved to be unsatisfactory.

INTRODUCTION

In the past, harbours and marinas of various shapes and sizes have often been known to possess poor water quality characteristics, caused chiefly by internal stagnant regions known to dominate within the harbour. Historically though, the quality of water within harbours and marinas has been assumed, in part, to be dependent upon the basin's flushing rates and human activity on or adjacent to the basin. The natural engineering solution to this water quality problem is either to design the harbour initially such that the planform geometry produces a maximum flushing efficiency or, if the harbour has already been constructed, to alter the planform geometry favourably by modifying the boundary shape or inserting shear walls where appropriate.

Although a number of laboratory model studies have been carried

* Lecturer in Civil Engineering, University of Birmingham, Birmingham, England.

out for particular harbours and marinas (e.g. Nece and Richey (1,2)), where the main objective has been to determine the ideal boundary shape tending to produce a maximum overall flushing efficiency in the model, little use of numerical models appears to have been made in this type of analysis. This is possibly due to the generally complex nature of the velocity fields resulting from narrow entrances associated with harbours and marinas. The complexity of the velocity fields occurs in the form of separation streamlines around harbour entrances, and the resulting non-uniform properties of the flow, particularly on the incoming tide. This paper describes such a numerical model which has been specifically developed to predict the depth averaged velocities and concentrations in narrow entranced harbours and marinas.

The time dependent equations of mass, momentum and solute transport have been expressed in a two time level alternating direction implicit finite difference form, with the effects of bottom roughness and turbulent momentum transfer being included. The stability problems generally associated with the non-linear convective accelerative terms, particularly for the type of velocity fields being considered, have been overcome by time centring these terms with respect to the remaining velocity derivatives (3). The apparent favourable numerical properties of this difference scheme have been partially confirmed by applying the Fourier series stability method to a quasi-linearised one-dimensional form of the appropriate equations (4).

The numerical model has been applied to an idealised prototype rectangular harbour with an asymmetric entrance, a constant planform area and varying length to breadth ratios. The geometric dimensions of this harbour, together with the mean depth and tidal wave properties, were assumed to be similar to many existing and proposed basins in Puget Sound of the State of Washington. The resulting depth averaged velocity fields and mean concentration distributions, determined for each length to breadth ratio, were then compared to the corresponding observed path-lines and measured exchange coefficients for two independent hydraulic model studies (5,6). Also numerical and laboratory model tests and comparisons were carried out to determine the influence on the flushing efficiency of the insertion of impermeable barriers at selected locations within the harbour geometries considered.

GOVERNING DIFFERENTIAL EQUATIONS

The appropriate two-dimensional differential equations governing the tide induced fluid and concentration movements within harbours and marinas can be derived by integrating, over the depth, the standard equations of continuity, momentum and mass transport. For an incompressible turbulent fluid on a rotating earth, the depth averaged equations of horizontal motion can be expressed in Cartesian co-ordinate form as:

$$\frac{\partial U}{\partial t} + \frac{\alpha}{(h+\eta)}\left[\frac{\partial U^2(h+\eta)}{\partial x} + \frac{\partial UV(h+\eta)}{\partial y}\right] - fV + g\frac{\partial \eta}{\partial x} + \frac{gU\sqrt{U^2+V^2}}{(h+\eta)C^2} - \varepsilon\left[\frac{\partial^2 U}{\partial x^2} + \frac{\partial^2 U}{\partial y^2}\right] = 0 \qquad \ldots\ldots\ldots (1)$$

$$\frac{\partial V}{\partial t} + \frac{\alpha}{(h+\eta)}\left[\frac{\partial VU(h+\eta)}{\partial x} + \frac{\partial V^2(h+\eta)}{\partial y}\right] + fU + g\frac{\partial \eta}{\partial y}$$

$$+ \frac{gV\sqrt{U^2+V^2}}{(h+\eta)C^2} - \varepsilon\left[\frac{\partial^2 V}{\partial x^2} + \frac{\partial^2 V}{\partial y^2}\right] = 0 \qquad \ldots\ldots\ldots (2)$$

where U,V = depth average velocities in x,y directions respectively, α = velocity correction factor = 1.016 for seventh power law velocity distribution, h = mean depth, η = water surface elevation above or below mean depth, f = Coriolis parameter, g = gravitational acceleration, C = Chezy roughness coefficient and ε = depth mean eddy viscosity = $1.154\, g(h+\eta)\sqrt{U^2+V^2}/C^2$ for seventh power law velocity distribution. Similarly, the equations of continuity and mass transport can be written as, respectively:

$$\frac{\partial \eta}{\partial t} + \frac{\partial U(h+\eta)}{\partial x} + \frac{\partial V(h+\eta)}{\partial y} = 0 \qquad \ldots\ldots\ldots (3)$$

$$\frac{\partial S(h+\eta)}{\partial t} + \frac{\partial S(h+\eta)}{\partial x} + \frac{\partial S(h+\eta)}{\partial y} = \frac{\partial}{\partial x}\left[D_x(h+\eta)\frac{\partial S}{\partial x}\right]$$

$$\frac{\partial}{\partial y}\left[D_y(h+\eta)\frac{\partial S}{\partial y}\right] \qquad \ldots\ldots\ldots (4)$$

in which S = depth mean mass concentration and D_x, D_y = depth mean dispersion coefficients where, from Elder (7), it is assumed that $D_x = (5.93|U| + 0.23|V|)\sqrt{g(h+\eta)}/C$, and similarly for D_y where the U and V velocities are interchanged.

In addition to these differential equations, various boundary conditions had to be included in the numerical model. For the closed boundaries it was assumed that the normal velocity components and the advective and diffusive transport of concentrations were all zero. Likewise, for the open boundary conditions, it was assumed that the incoming tidal wave was sinusoidal in form, whereby:

$$\eta = a\,\mathrm{Cos}\,(\omega t + \emptyset) \qquad \ldots\ldots\ldots (5)$$

with a = wave amplitude, ω = wave frequency, t = time and $\emptyset$ = phase lag; and that the velocity components at the harbour entrance, were given by the simplified form of the continuity equation:

$$U = A\frac{d\eta}{dt}\Big/W(h+\eta) \qquad \ldots\ldots\ldots (6)$$

where A = harbour planform area and W = harbour entrance width. For the concentration values at the harbour entrance, these were assumed to be the same as those for the open sea on the incoming tide, whilst on the outgoing tide values were determined from those predicted within the harbour by linear interpolation.

FINITE DIFFERENCE EQUATIONS

The differential equations (1) - (4) were expressed in an alternating direction implicit finite difference form, with all terms being fully centred in both space and time, except for the pressure gradients in the momentum equations. Using the space staggered grid scheme shown in Fig. 1, then for the first half time-step n, U and S were implicitly solved for using the following finite difference forms of the continuity, x-direction momentum and mass transport equations respectively:

$$\eta^{n+\frac{1}{2}}_{j,k} = \eta^{n}_{j,k} - \frac{\Delta t}{2\Delta x}\left[(h+\eta)U\Big|^{n+\frac{1}{2}}_{j+\frac{1}{2},k} - (h+\eta)U\Big|^{n+\frac{1}{2}}_{j-\frac{1}{2},k} + (h+\eta)V\Big|^{n-1}_{j,k+\frac{1}{2}} - (h+\eta)V\Big|^{n-1}_{j,k-\frac{1}{2}}\right] \quad \ldots\ldots\ldots (7)$$

$$U^{n+\frac{1}{2}}_{j+\frac{1}{2},k} = U^{n-3/2}_{j+\frac{1}{2},k} - \frac{2\alpha\Delta t}{\Delta x}\left[U^2\Big|^{n-\frac{1}{2}}_{j+1,k} - U^2\Big|^{n-\frac{1}{2}}_{j,k} + UV\Big|^{n-\frac{1}{2}}_{j+\frac{1}{2},k+\frac{1}{2}} - UV\Big|^{n-\frac{1}{2}}_{j+\frac{1}{2},k-\frac{1}{2}}\right]$$

$$- \frac{2\Delta tg}{\Delta x}\left(\eta^{n+\frac{1}{2}}_{j+1,k} - \eta^{n+\frac{1}{2}}_{j,k}\right) - \frac{\Delta tg(U^{n+\frac{1}{2}} + U^{n+3/2})\sqrt{U^2+V^2}}{(h+\eta)C^2}\Big|^{n-\frac{1}{2}}_{j+\frac{1}{2},k}$$

$$+ \frac{2\varepsilon\Delta t}{\Delta x^2}\left[U^{n-\frac{1}{2}}_{j+3/2,k} + U^{n-\frac{1}{2}}_{j+\frac{1}{2},k+\frac{1}{2}} - 2\left(U^{n+\frac{1}{2}}_{j+\frac{1}{2},k} + U^{n-3/2}_{j+\frac{1}{2},k}\right) + U^{n-\frac{1}{2}}_{j+\frac{1}{2},k-\frac{1}{2}} + U^{n-\frac{1}{2}}_{j-\frac{1}{2},k}\right] \quad \ldots\ldots\ldots (8)$$

$$[S(h+\eta)]^{n+\frac{1}{2}}_{j,k} = [S(h+\eta)]^{n}_{j,k} - \frac{\Delta t}{2\Delta x}\left[S(h+\eta)U\Big|^{n+\frac{1}{2}}_{j+\frac{1}{2},k} - S(h+\eta)U\Big|^{n+\frac{1}{2}}_{j-\frac{1}{2},k} + S(h+\eta)V\Big|^{n}_{j,k+\frac{1}{2}} - S(h+\eta)V\Big|^{n}_{j,k-\frac{1}{2}}\right] - \frac{\Delta t}{2\Delta x^2}\left[(S_{j+1,k} - S_{j,k})(h+\eta)D_x\Big|^{n+\frac{1}{2}}_{j+\frac{1}{2},k} - (S_{j,k} - S_{j-1,k})(h+\eta)D_x\Big|^{n+\frac{1}{2}}_{j-\frac{1}{2},k} + (S_{j,k+1} - S_{j,k})(h+\eta)D_y\Big|^{n}_{j,k+\frac{1}{2}} - (S_{j,k} - S_{j,k-1})(h+\eta)D_y\Big|^{n}_{j,k-\frac{1}{2}}\right] \quad \ldots\ldots\ldots (9)$$

where j,k = finite difference grid co-ordinates in x,y directions respectively, and n = time-step level. For the second half time-step, from level $n+\frac{1}{2}$ to $n+1$, similar equations were formulated with η,V and S written and solved for in an implicit form, whilst terms involving U

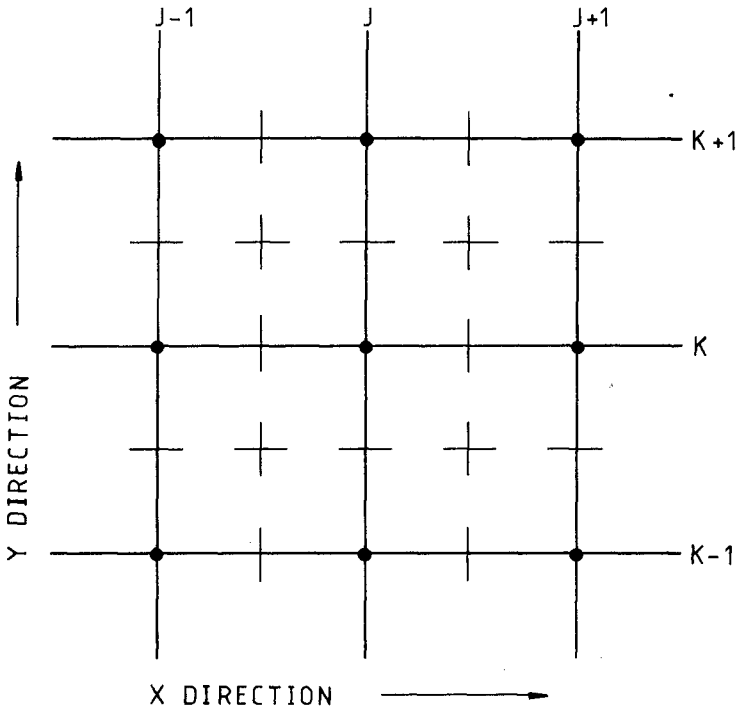

Symbols

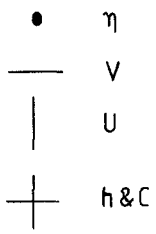

Fig. 1 The Finite Difference Grid

were expressed explicitly.

This finite difference representation of the original differential equations has a truncation error of order Δt, Δx^2 and with the only stability constraint being introduced by the convective accelerative terms (4) as:

$$\frac{\alpha \Delta t}{\Delta x} \left| U_{max} \right| \leq 1 \qquad \ldots\ldots\ldots (10)$$

For the type of velocity fields being considered, where the maximum velocity U_{max} is relatively small, this stability constraint poses little restriction on the numerical model, particularly in comparison to the accuracy requirements suggested by Vreugdenhil and Voogt (8) as:

$$\frac{\Delta t}{\Delta x} \sqrt{gh} \leq 5 \qquad \ldots\ldots\ldots (11)$$

The finite difference equations were solved using the method of Gaussian elimination and back substitution and were found to give numerically stable results for all harbour configurations considered.

APPLICATION OF MODEL

In an attempt to check the reliability of the numerical model, comparisons were made with the results obtained from two laboratory model studies (5,6), carried out prior to the final development of the numerical model. In both of these experimental studies the main objectives were to compare the flushing characteristics and velocity fields for a number of different model rectangular harbour shapes. Each harbour shape had a different length to breadth ratio, but in all cases the harbour planform area remained constant. By comparing the flushing characteristics for the different shapes, it was possible to conclude which shape induced the maximum tidal flushing efficiency and hence, in general, resulted in the best overall water quality characteristics. Tests were also carried out to study the effects of inserting impermeable barriers at various locations within the different harbours, to investigate whether or not the flushing characteristics could be improved by altering the planform geometry accordingly.

The laboratory studies were treated as model studies of idealized harbour shapes, typical of many existing and proposed harbours and marinas in Puget Sound of the State of Washington. In the latter of the two laboratory studies in particular, where the experimental results were more directly comparable with the numerical model results, the prototype harbour was assumed to have a planform area of 4.0×10^5 m^2, a mean depth of 6.0 m an an asymmetric entrance of width 128.0 m. Also the prototype semi-diurnal tides, of period 12.4 hr., were assumed to be sinusoidal with an amplitude of 1.5 m. In the laboratory model the horizontal and vertical length scales were 1:1000 and 1:50 respectively, giving a vertical distortion of 20:1, with a Froude law scaling relationship being used to model the tidal period. The resulting physical model had a planform area of 0.4 m^2, a mean depth of 120 mm, an entrance width

of 128 mm, a wave amplitude of 20 mm and a period of 10.52 min, see Fig. 2. The variable length to breadth ratios (L/B) considered ranged from 0.33 to 3.00, where the length L was defined as the harbour width in the plane of the entrance and the breadth B as the width perpendicular to the entrance plane.

Although vertically distorted hydraulic models do not properly scale diffusion and dispersion processes (9), the assumption was made that the dominant mode of water exchange was by convective, rather than diffusive or dispersive, transport. This allowed tracer dyes to be used in the model and for this purpose rhodamine B was used.

For the laboratory tests the harbour model, with adjustable sidewalls, was inserted into a tidal tank in which an oscillating weir reproduced the required model tides (Fig. 2). With the harbour sidewalls set at the required length to breadth ratio, the tank and harbour were filled to the low tide water level and the harbour entrance temporarily sealed. Using a hypodermic syringe, 75 ml of rhodamine B (concentration 7.5 mg/l) was then thoroughly mixed with the harbour water and the average initial concentration recorded using a fluorimeter. The temporary entrance barrier was then removed and the tidal generator run for a period of three complete tidal cycles, at the end of which the harbour entrance was re-sealed. The fluid enclosed within the harbour was again thoroughly mixed and the average final concentration recorded as before. Knowing both the initial and final spatially averaged concentrations within the harbour, and the number of tidal cycles, then the average per cycle exchange coefficient was determined from the relationship given by Nece and Richey (2):

$$E = 1 - (C_i/C_o)^{1/i} \qquad \ldots\ldots\ldots (12)$$

where E = average per cycle exchange coefficient, C_o = initial concentration and C_i = final concentration after i tidal cycles. The experimentally measured exchange coefficients for the various L/B ratios considered are given in Fig. 3, where it can be seen that the maximum value, resulting in the maximum flushing efficiency, occurs for an L/B ratio of unity i.e. a square harbour.

After measuring the exchange coefficient for each L/B ratio, the tide induced circulation patterns were determined using weighted drinking straws as drogues. The tidal generator was first run for two complete tidal cycles and on the third cycle the drogues were carefully inserted at fixed points, one minute before the flood and ebb mean tide water levels, and were then tracked for two minutes. The resulting pathlines were plotted to scale giving an indication of the corresponding velocity fields. Two sample results are shown for L/B ratios of 1.0 and 1.8 respectively, see Figs. 4 and 5.

In a similar procedure to that adopted for the laboratory model studies, the numerical model was applied to the prototype harbour with the planform area, mean depth and entrance width being as before, i.e. 4.0×10^5 m^2, 6.0 m and 128.0 m respectively. Likewise the semi-diurnal sinusoidal tides had a period of 12.4 hr and an amplitude of 1.5 m. The model was started from the low water level, with an initial state of

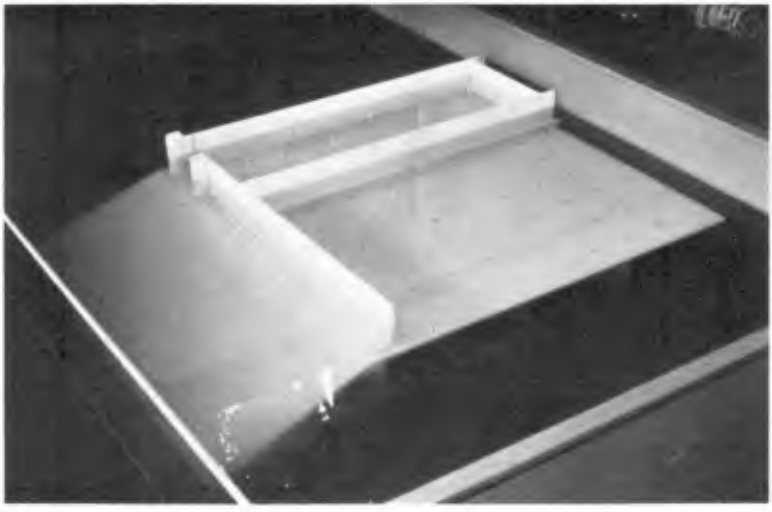

Fig. 2 General View of the Laboratory Model

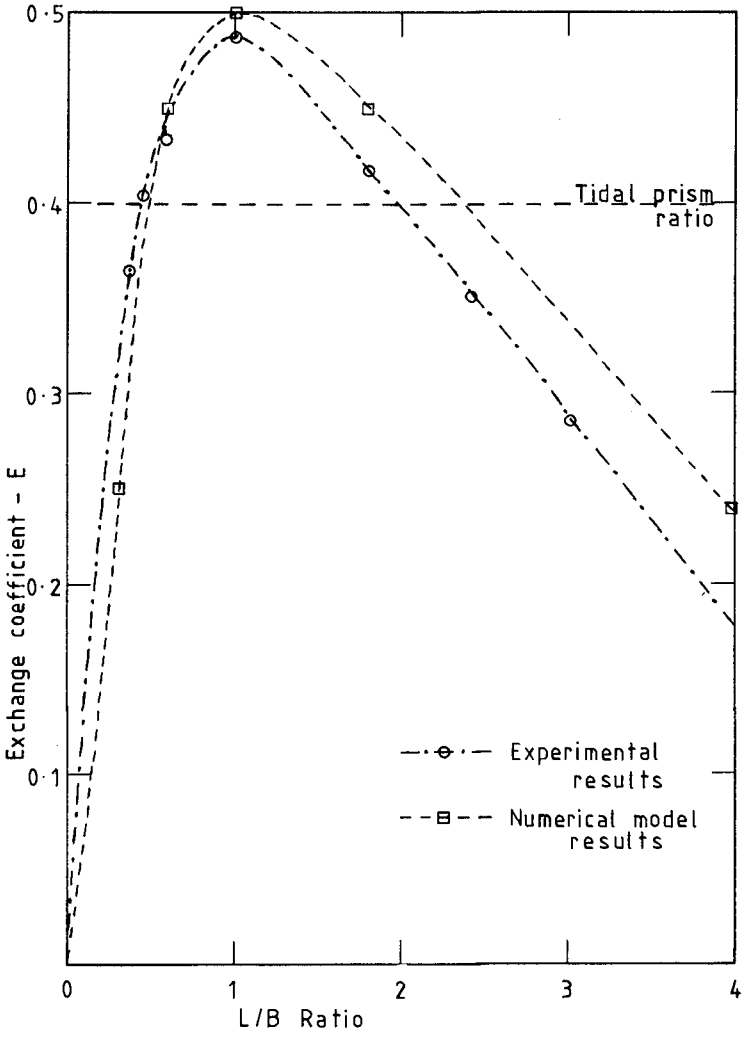

Fig. 3 Variation of Exchange Coefficient E with L/B Ratio

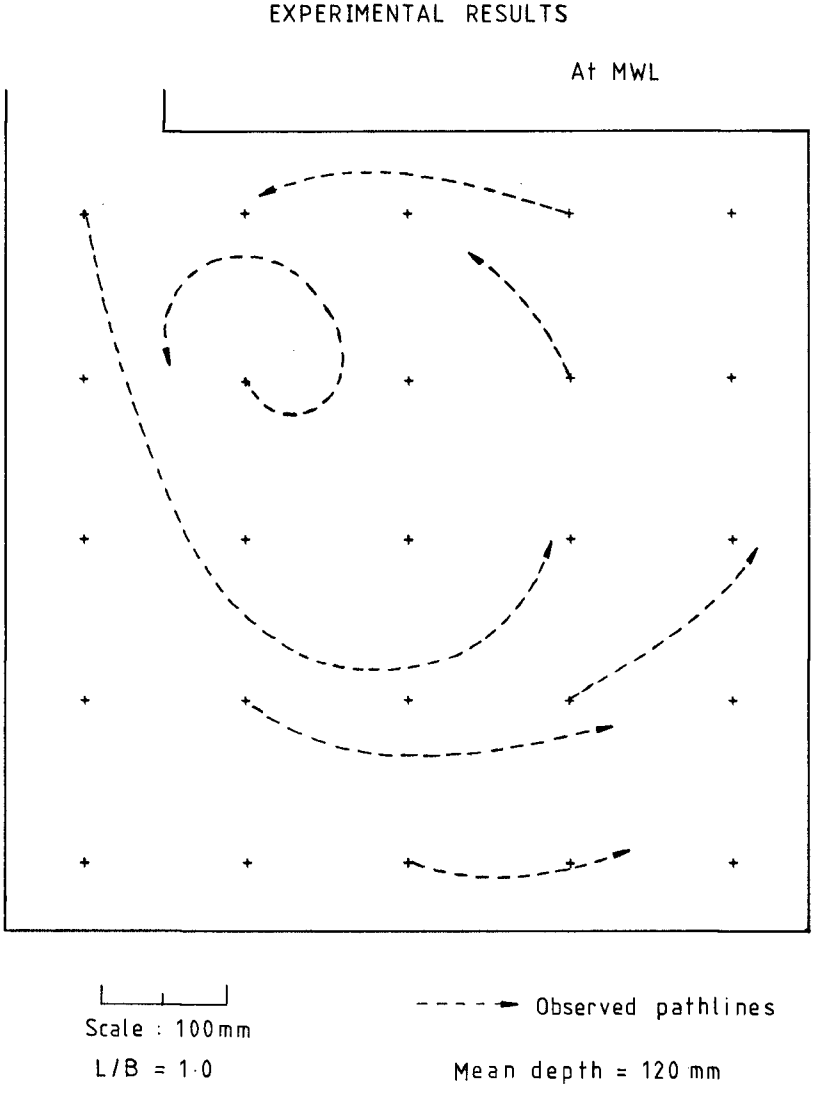

Fig. 4 Experimentally Observed Pathlines for L/B Ratio of 1.0

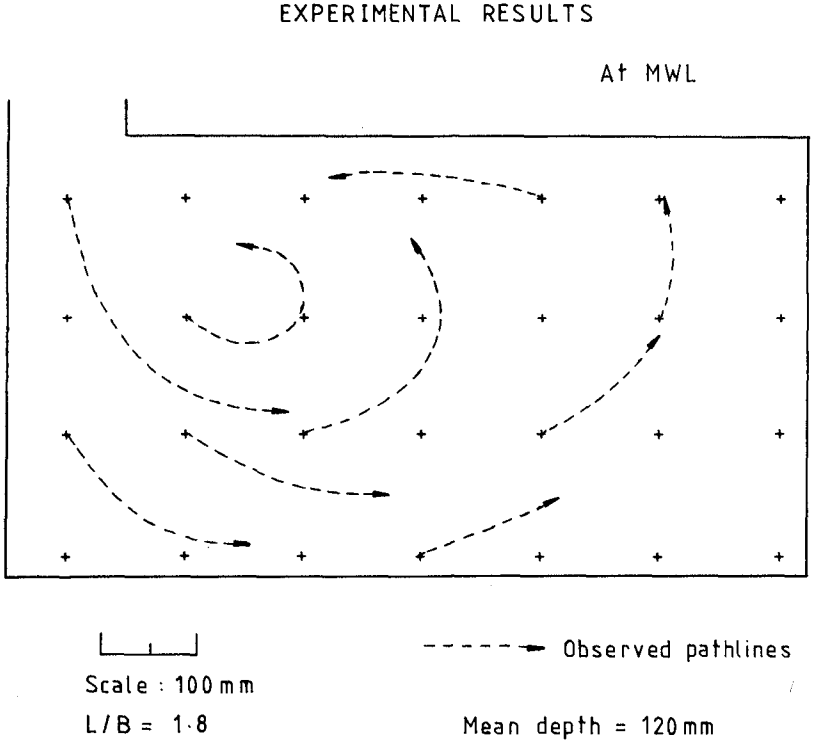

Fig. 5 Experimentally Observed Pathlines for L/B Ratio of 1.8

rest being assumed within the harbour. Also at the start of the model, the initial concentration (C_0) at each grid point within the domain was assumed to be 50 ppm. As for laboratory model studies, varying L/B ratios were considered ranging from 0.25 to 4.0; the range of values being larger in this study since no restraints were imposed by physical space requirements.

For all the L/B ratios considered the numerical model was run for three tidal cycles with the spatially averaged concentration (C_j) being calculated at the end of this period. As for the experimental results, the average per cycle exchange coefficient was evaluated using Eq. (12), with the results being given in Fig. 3. The agreement between the numerical and experimental results is encouraging, with the general trends of the relationship between the exchange coefficient and the L/B ratio being almost identical. In both cases the maximum exchange coefficient occurs for a square harbour, indicating as before that this shape induces the best flushing characteristics.

Graphical representations of the numerically predicted velocity fields were reproduced at the mean flood and ebb tides, thus allowing a direct comparison with the experimental results for the third tidal cycle. Again the agreement between the numerical and experimental results proved encouraging, with the general features of the tide induced circulation being satisfactorily reproduced. As an example of the numerical model results, the velocity fields are shown for L/B ratios of 1.0 and 1.8 respectively, see Figs. 6 and 7. These examples correspond directly to the experimental results of Figs. 4 and 5.

A further feature of the numerical model was that the variation of concentration across the planform area of the harbour was determined at particular time levels. By evaluating the standard deviation of concentration, and dividing by the average concentration, the corresponding coefficient of concentration variation was obtained. The results determined for the various L/B ratios, with and without the inclusion of barriers in the model, can be seen in Fig. 8. The results have again confirmed that an L/B ratio of unity provides the best mixing characteristics. For this case the lowest coefficient of variation was obtained, which meant that the concentration was more uniformly mixed within the harbour than for the other L/B ratios.

Further tests were carried out, both for the laboratory and numerical models, to study the effects on the gross flushing characteristics of inserting impermeable barriers at various positions within the harbours. Although the results are not reproduced here, it has been confirmed from both the experimental and numerical results that barriers do not in any way improve the flushing characteristics. In fact, the results recorded clearly showed that the barriers had a detrimental effect on the flushing efficiency.

CONCLUSIONS

It has been shown that by representing the differential equations of continuity, momentum and mass transport in the finite difference form described, numerically stable solutions can be obtained for the

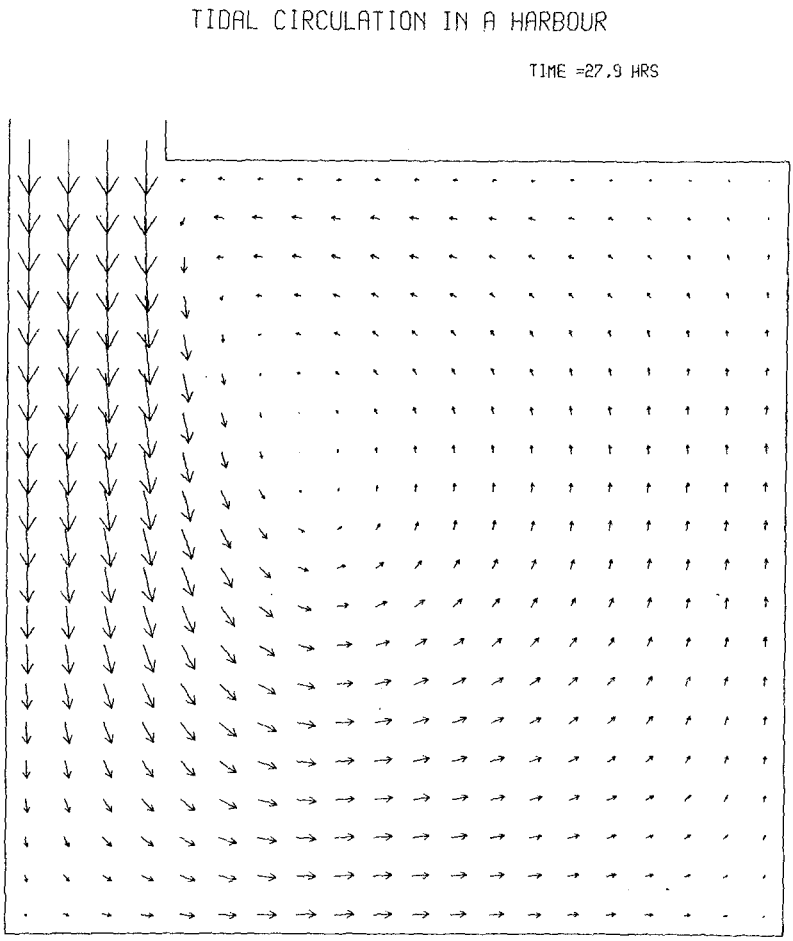

Fig. 6 Computed Velocity Field and Concentration Parameters for L/B Ratio of 1.0

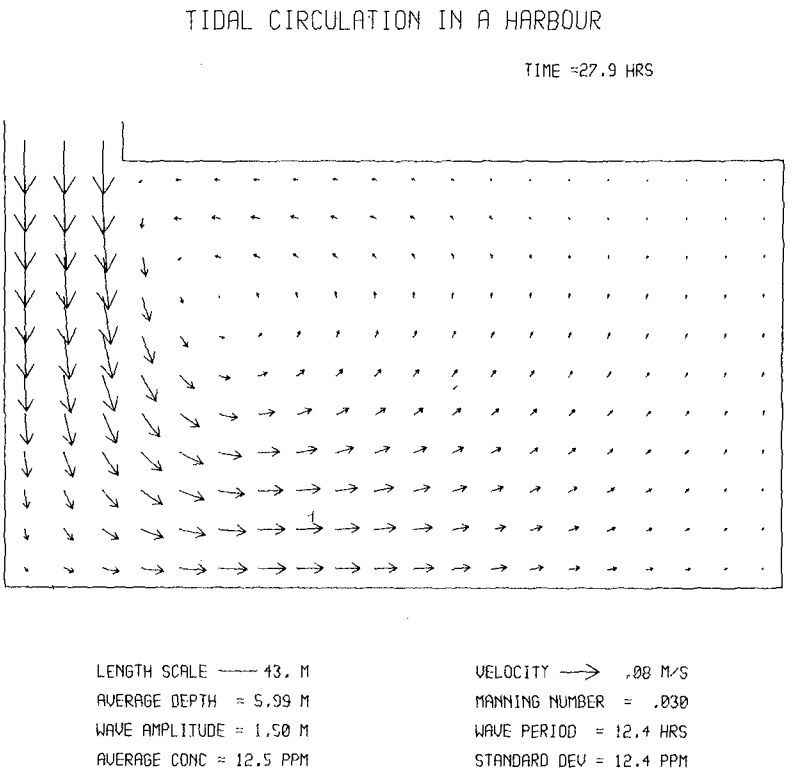

Fig. 7 Computed Velocity Field and Concentration Parameters for L/B Ratio of 1.3

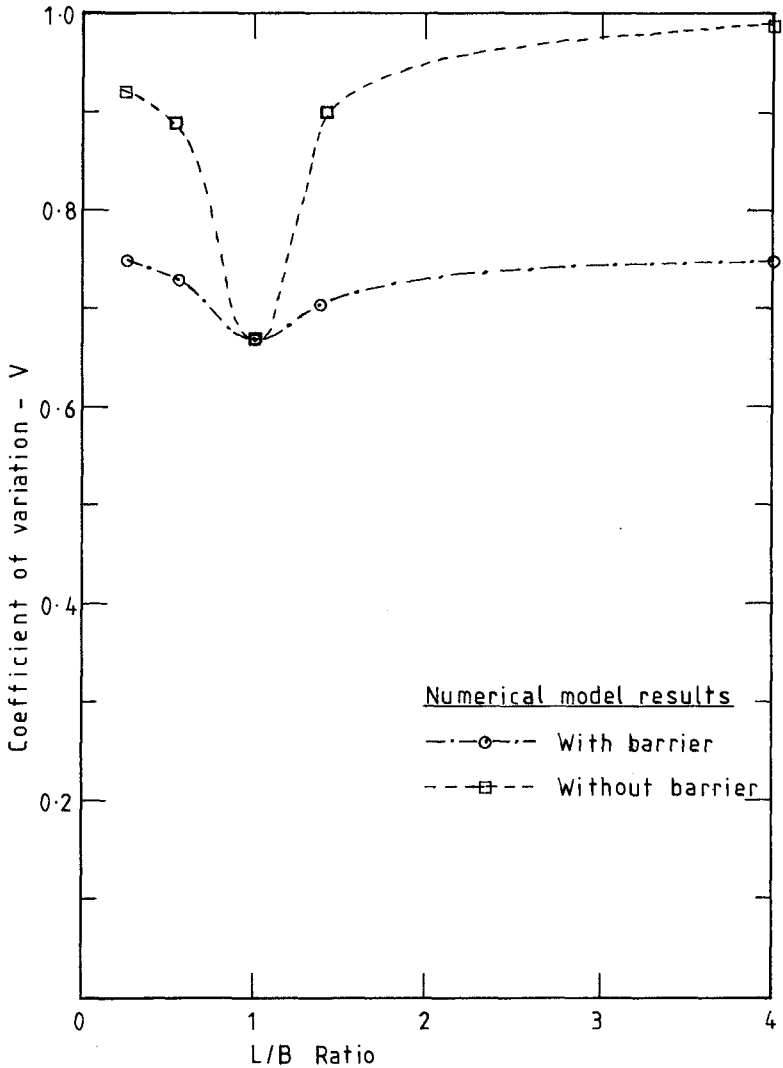

Fig. 8 Variation of Concentration Distribution with L/B Ratio

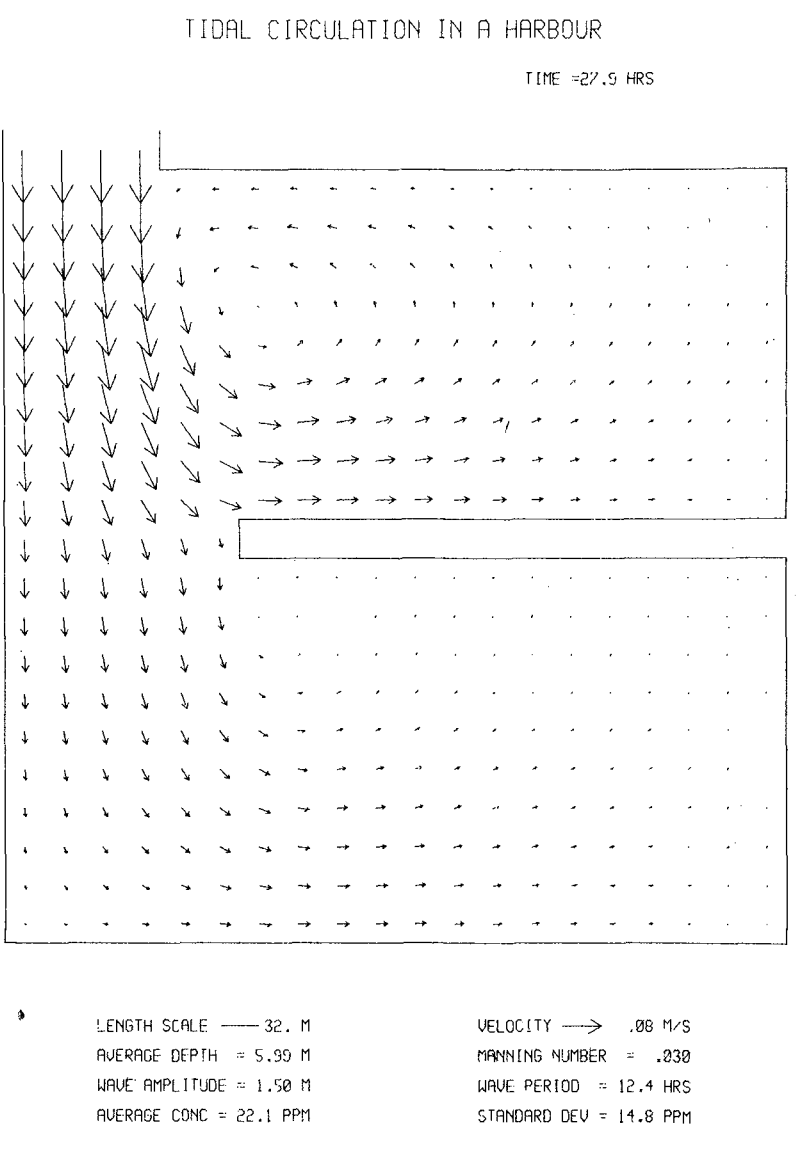

Fig. 9 Computed Velocity Field and Concentration Parameters for L/B of 1.0 with Barrier Included

relatively complex flow fields considered. This representation includes time centring of the convective accelerations, a technique which appears to have overcome the problems generally associated with non-linear instabilities. In all of the comparisons made between the numerical model velocity field predictions and the experimentally observed path-lines, the results have agreed reasonably well with the essential characteristics of the flowfields having been adequately reproduced.

By determining the spatially averaged concentrations at the beginning and end of three tidal cycles, it has been possible to ascertain the average per cycle exchange coefficient for various L/B ratios in the laboratory and numerical models. Comparisons of the results again showed good agreement, with the peak exchange coefficient occurring for an L/B ratio of unity; thus indicating that a square harbour gives the maximum flushing efficiency for a constant planform area.

For the numerical model studies only, results were obtained for the concentration distributions across the harbour planform area. As before these results indicated that for a square harbour the plan variation of the concentration distribution was a minimum, thereby confirming that for this case the concentrate was more uniformly mixed within the basin.

Finally, velocity field predictions and exchange coefficients for both the laboratory and numerical model results, showed that the insertion of impermeable barriers within the harbours was detrimental to the improvement of the basin's flushing efficiency and overall water quality characteristics.

REFERENCES

1. Nece, R.E. and Richey, E.P., "Flushing Characteristics of Small-Boat Marinas", Proceedings of the Thirteenth Coastal Engineering Conference, Vancouver, Canada, July 1972, pp 2499-2512.

2. Nece, R.E. and Richey, E.P., "Application of Physical Tidal Models in Harbor and Marina Design", Proceedings of the Symposium on Modeling Techniques, ASCE, San Francisco, California, September 1975, pp 783-801.

3. Falconer, R.A., "Numerical Modelling of Tidal Circulation in Harbours", Journ. of the Waterway, Port, Coastal and Ocean Division, ASCE, Vol. 106, No. WW1, February 1980, pp 31-48.

4. Falconer, R.A., "Mathematical Modelling of Jet-Forced Circulation in Reservoirs and Harbours", Ph.D. Thesis, University of London, London, England, 1976, 237 pp (unpublished).

5. Falconer, R.A., "Tidal Circulation Effects in Rectangular Harbors", MSCE Thesis, University of Washington, Seattle, Washington, 1974, 97pp (unpublished).

6. Roberts, K. and Withycombe, S.I., "Tidal Flushing Characteristics of Rectangular Harbours", B.Sc. Thesis, University of Birmingham, Birmingham, England, 1980, 56 pp (unpublished).

7. Elder, J.W., "The Dispersion of Marked Fluid in Turbulent Shear Flow", Journ. of Fluid Mechanics, Vol. 5, Part 4, 1959, pp 544-560.

8. Vreugdenhil, C.B. and Voogt, J., "Hydrodynamic Transport Phenomena in Estuaries and Coastal Waters", Proceedings of the Symposium on Modeling Techniques, ASCE, San Francisco, California, September 1975, pp 690-708.

9. Harleman, D.R.F., "Pollution in Estuaries", Chapter 14 in Estuary and Coastline Hydrodynamics (A.T. Ippen, Ed.), McGraw-Hill, 1966.

NOTATION

a	=	wave amplitude
A	=	planform area of harbour
B,L	=	breadth and length of harbour respectively
C	=	Chezy coefficient
C_o, C_i	=	initial and final concentrations in harbour respectively
D_x, D_y	=	depth mean dispersion coefficients in x,y directions respectively
E	=	exchange coefficient
f	=	Coriolis parameter
g	=	acceleration due to gravity
h	=	mean depth
i	=	number of tidal cycles
j,k	=	finite difference co-ordinates in x,y directions respectively
n	=	time-step level
S	=	depth mean mass concentration
U,V	=	depth mean velocities in x,y directions respectively
W	=	entrance width of harbour
x,y	=	longitudinal and lateral co-ordinates respectively
α	=	vertical velocity variation correction factor
Δt	=	time step
Δx	=	grid size in x,y directions
ε	=	depth mean eddy viscosity
$\emptyset$	=	phase lag
ω	=	wave frequency